CELL SEGMENTATION VIA REGION-BASED ELLIPSE FITTING

Costas Panagiotakis[1,2] *and Antonis A. Argyros*[1,3]

[1]Institute of Computer Science, FORTH, Greece
[2]Business Administration Department (Agios Nikolaos), TEI of Crete, Greece
[3]Computer Science Department, University of Crete, Greece
Email: {cpanag,argyros}@ics.forth.gr

ABSTRACT

We present a region based method for segmenting and splitting images of cells in an automatic and unsupervised manner. The detection of cell nuclei is based on the Bradley's method. False positives are automatically identified and rejected based on shape and intensity features. Additionally, the proposed method is able to automatically detect and split touching cells. To do so, we employ a variant of a region based multi-ellipse fitting method that makes use of constraints on the area of the split cells. The quantitative assessment of the proposed method has been based on two challenging public datasets. This experimental study shows that the proposed method outperforms clearly existing methods for segmenting fluorescence microscopy images.

Index Terms— Nuclei Segmentation, Ellipses Fitting, Shape Analysis, Bradleys method.

1. INTRODUCTION

The automatic image segmentation is a key step in many image/video analysis tasks and multimedia applications [1, 2]. In this work, we study the problem of accurate image segmentation of cells in fluorescence microscopy images, which plays a key role in high-throughput applications such as quantification of protein expression and the study of cell function [3]. Figure 1 depicts a fluorescence microscopy image showing cells that are heterogeneous in shape and size. The image exhibits considerable foreground and background intensity variations. The ground truth centroid of each cell is shown with a red plus. The boundaries detected by the proposed method are plotted in green color and are in almost full agreement with the ground truth, although there exists several cases of touching cells.

Related work: Cell segmentation can be addressed by interactive segmentation techniques. However, interactive/manual cell segmentation is a subjective, tedious, labor-intensive, and time-consuming task, especially for large datasets. Therefore, automatic cell segmentation methods with the ability to deal with different cell types and image artifacts are required [3, 4].

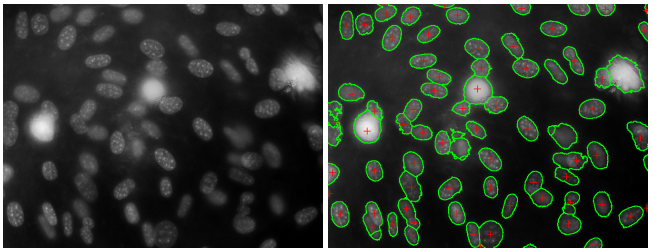

Fig. 1. A fluorescence microscopy image (left) and the output of the proposed method (right). The boundaries of the detected cells and of the ground truth cell centroids are plotted with green curves and red pluses, respectively.

Several image segmentation methods have been proposed to automatically detect and spit overlapping cells in fluorescence microscopy images. Most of the methods consist of two main steps, (a) image segmentation for detecting cells and cell constellations and (b) splitting of overlapping cells.

A method that is often used as an initialization step in cell segmentation and detection is the Otsu's method [5, 6, 7, 4, 8] that performs fully automatic clustering-based image thresholding. This method assumes that there exist two classes of pixels, foreground (cell) pixels and background. It calculates the optimum threshold separating the two classes so that their combined spread (intra-class variance) is minimal. The Otsu's method does not perform sufficiently well when the assumption for two classes is violated, as it happens when there is considerable intensity inhomogeneity in the image foreground and/or background (e.g., see Fig. 1). This problem is also common to other segmentation methods that compute global thresholds for detecting cells [9].

Deformable models, which are able to capture a wide spectrum of different shapes, can also be considered as another category of cell segmentation techniques [3]. There are two main types of deformable models: parametric models, which use an explicit representation of objects and implicit models like level sets. Level sets methods [10, 11, 4] have been used to extract contours and to evaluate whether a cell is

blurry. Such methods show promising results, but they usually require initialization e.g., by Otsu's method as proposed in [4].

The splitting of touching cells is often handled with watershed-based segmentation [12, 13]. However, such methods suffer from over-segmentation when cells have different sizes and shapes [6]. The over-segmentation is reduced in [13] using marker-controlled watersheds, but the detection of markers is still not accurate in cases of considerable overlap of the cells [4]. In [3], touching cells are first distinguished from non-touching ones based on predefined rules applied to the convex hull of the segmented cell regions. Then splitting is achieved by identifying splitting point-pairs. In [9], the splitting is done by minimizing the maximum eccentricity of the resulting sub-regions under the constraint of equal cells area. This results in equally sized cells of almost circular shape.

Many recent methods [4, 6, 8, 14] operate by fitting ellipses to the boundaries of segmented cells, or to specific proper boundary split points. These methods give promising results when the segmentation method identifies accurately the boundaries of the cell regions. However, they are sensitive to errors on boundary detection and they rely on heuristically determined thresholds to identify the splitting points of the touching cells. Curvature estimation can be also used for cell splitting [6, 8, 15], but such methods share the aforementioned robustness issues that are common to the rest of the boundary-based methods.

Our contribution: This work proposes a region-based method that makes several contributions to the problem of accurate cell segmentation. First, we have modified the Bradleys segmentation method [16], which is a real-time adaptive thresholding method that exploits the mean intensity is a local window. The Bradleys method is selected because it is local and adaptive and performs well in challenging images with intensity inhomogeneity. In addition, to split the touching cells with high accuracy, we applied an extension of the Decremental Ellipse Fitting Algorithm (DEFA) [17] which performs region-based ellipse fitting. DEFA has several advantages over other existing methods:

- It is a parameter free method.
- It is a region-based method. As such, it is considerably more robust and tolerant to noise and boundary segmentation errors than boundary-based methods.
- There is no need for an explicit, extra step to detect the touching cells, because DEFA automatically identifies them.
- DEFA identifies automatically the number of cells by considering different models (i.e., solutions involving different numbers of ellipses) and evaluating them based on the Akaike Information Criterion (AIC).

In summary, the main contributions of this paper are:

- The improvement of Bradleys segmentation method, taking into account shape and intensity features and the use of Voronoi diagram to compute local background intensity features.
- The use of DEFA, an efficient, region based, parameter-free ellipse fitting method [17] to automatically detect and split touching cells. The proposed splitting method is able to accommodate shape-based constraints to automatically reject spurious splitting solutions.
- The experimental, quantitative evaluation of the propose method based on standard datasets which shows that it outperforms existing, state of the art methods.

2. THE SEG-SELF METHOD

We present the proposed method for cell segmentation and splitting based on ellipse fitting, called *SEG-SELF*.

2.1. Image Segmentation

We assume a gray-scale image (see Fig. 1) containing a number of cells that may vary with respect to size and shape and which may be touching each other. The cells may vary in brightness. This may also be true for the cell's background. Each cell is free of holes and can be discriminated from its local background because of its higher brightness and its elliptic-like shape.

The first step in our approach is to apply the Bradley's segmentation method [16] and a hole filling step. The Bradley's method calculates a locally adaptive image threshold that is chosen based on local, first-order image statistics around each pixel. This method is robust to illumination changes and clearly outperforms global thresholding techniques like Otsu's method [5] in images that exhibit high illumination variations. A drawback of Bradley's method is that, segments of the background with locally higher brightness, are erroneously identified as cells (see Figure 2(b)). To reduce these false positives, we have introduced two shape- and one appearance-based constraints.

Area constraint (shape): The expected area of each cell should exceed a minimum threshold, T_α. So, segments that are particularly small, are rejected from further consideration. To avoid the rejection of cells that are partially visible (i.e., appear at/intersect with image boundaries), T_α is not applied to the measured object area, but rather to an approximation of their *expected* area. This is computed as the area of the circle that can be fitted best to the eight extrema points of their boundary [18].

Roundness constraint (shape): Cells are circular/elliptic-like objects, so we have used the roundness measure to reject objects with complex shapes that deviate considerably

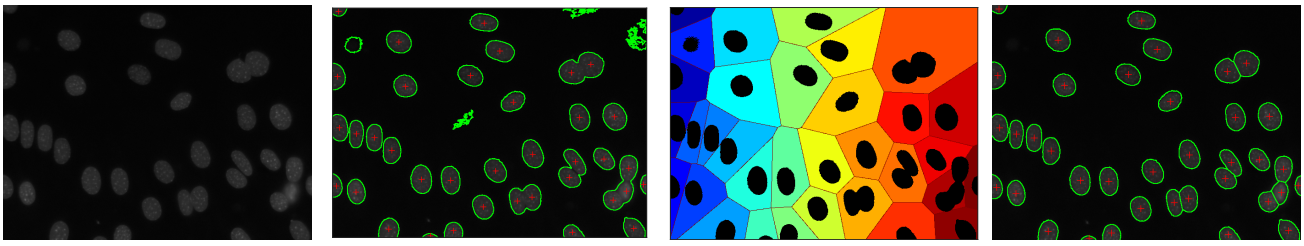

(a) (b) (c) (d)

Fig. 2. **(a)** A fluorescence microscopy image. **(b)** The boundaries of the detected cells according to the Bradleys segmentation method [16] projected on the given image. The cell centroids according to the ground truth data are plotted with red "+". **(c)** The local backgrounds of the detected cells according to the Voronoi diagram of their centroids. The detected cells are plotted in black. **(d)** Final result of the *SEG-SELF* method.

from this pattern. The Roundness R measures how closely the shape of an object resembles that of a perfect circle and is defined by the following ratio:

$$R = \frac{4\pi\alpha}{p^2}, \tag{1}$$

where α and p denote the area and the perimeter of the object, respectively. The roundness R takes a maximum value of 1 for the perfect circle. According to our experiments, for a region to actually represent a cell it is required that $R > 0.2$.

Intensity constraint (appearance): The aforementioned shape constraints suffice to reject several false positives as for example the one in the image center and the two in the top-right of Fig. 2(b). We introduce another, intensity-based constraint, that is uncorrelated to the shape-based constraints, to reject more false positives such as the circular object on the top right of Fig. 2(b). The intuition behind this constraint is that the intensity distribution within a cell should be more similar to the intensity distribution within the rest of the cells, rather than to the intensity distribution of the local background. To quantify this, we first extract the local background of each detected object by computing the Voronoi diagram of the objects' centroids and by removing from this the detected objects (see Fig. 2(c)). To measure the distance between two intensity distributions, we employ the popular Bhattacharyya distance [19, 20] under the assumption of normal distributions. More specifically, assuming two distributions q_1 and q_2, their means μ_i and their variances σ_i^2, $i \in \{1, 2\}$, the Bhattacharyya distance $D(q_1, q_2)$ of q_1 and q_2 is defined as [21]:

$$D(q_1, q_2) = \frac{1}{4}\left[ln\left(\frac{\sigma_1^2}{4\sigma_2^2} + \frac{\sigma_2^2}{4\sigma_1^2} + \frac{1}{2}\right) + \frac{(\mu_1 - \mu_2)^2}{\sigma_1^2 + \sigma_2^2}\right]. \tag{2}$$

Figure 2(b) shows the boundaries of the detected cells as those were identified by the original Bradley's segmentation method [16] superimposed to the input image and the ground truth as in Fig. 1. The four false positives are rejected by employing the proposed constraints (see Figure 2(d)).

2.2. Region Splitting

The aforementioned image segmentation step discriminates the foreground cells from their background. However, it cannot discriminate between touching cells. To do so, we apply a modified version of our previous work on region-based ellipse fitting (DEFA) [17] in each detected region of the previous step. The DEFA method approximates an arbitrary 2D shape with a number of ellipses. The number and the parameters of the ellipses are determined automatically under the constraint that the total area covered by the ellipses is equal to the area of the original shape. DEFA makes no assumption and requires no prior knowledge regarding the input shape.

DEFA operates as follows. First, the skeleton of the 2D shape is computed, which provides important information on the parameters of the ellipses that could approximate the original shape. DEFA starts with an automatically defined, large number of such ellipses (complex model) and progressively eliminates some of them (model simplification). Different models (i.e., solutions involving different numbers of ellipses) are evaluated based on the Akaike Information Criterion (AIC). This considers an entropy-based shape complexity measure that balances the model complexity and the model approximation error. DEFA may integrate constraints on the shape of the identified regions. In our problem, we setup DEFA to automatically reject regions whose area is less than T_α or the ratio between the largest splitted sub-region and the smallest one exceeds the value of 10. According to our experiments, this step reduces the over-segmentation by about 30%. Finally, the object's pixels are clustered into groups according to the detected ellipses, also keeping the detected boundaries of Bradley's segmentation method.

In principle, DEFA can be applied to all segments identified by the segmentation step described in Section 2.1. In practice, it suffices to apply DEFA in all regions whose area is greater than the median area of all detected regions. This results in a computational performance speed up of about 50% without sacrificing the quality of the obtained results.

Table 1. Segmentation results on the **U20S** dataset.

Methods	Jaccard	MAD	Hausdorff	DiceFP	DiceFN
Otsu	83.5	4.5	11.5	3.0	16.7
Three-step	88.4	4.7	13.4	5.3	5.2
LSBR	83.2	5.8	19.8	11.8	9.1
LLBWIP	**91.6**	3.5	12.7	**4.7**	**3.9**
SEG-SELF	89.3	**3.0**	**8.3**	**4.7**	6.8

Table 2. Segmentation results on the **NIH3T3** dataset.

Methods	Jaccard	MAD	Hausdorff	DiceFP	DiceFN
Otsu	56.9	6.2	12.9	24.2	35.4
Three-step	70.8	5.7	16.4	15.5	19.7
LSBR	64.2	7.2	19.8	21.2	20.4
LLBWIP	75.9	4.1	14.3	**12.7**	12.2
SEG-SELF	**80.8**	**3.7**	**8.8**	**12.7**	**9.0**

3. EXPERIMENTAL EVALUATION

The experimental evaluation of *SEG-SELF* involved its quantitative and qualitative assesment on standard datasets and in comparison with state of the art approaches.

The employed datasets: The experimental evaluation of the proposed method[1] was conducted using two public datasets that are annotated with ground truth, as presented in [22]:

- **U20S dataset**: A collection of 48 images (1349 $\times$ 1030 pixels) that include 1831 U20S cells.
- **The NIH3T3 dataset**: A collection of 49 images (1344 $\times$ 1024 pixels) that include 2178 NIH3T3 cels.

The NIH3T3 dataset is more challenging, since it contains cells/nuclei that vary greatly in brightness, and images often contain visible debris [22]. Both datasets show cells that are heterogeneous in shape and size.

Evaluation criteria: To assess the performance of segmentation, we employed both region-based and contour-based metrics, as in [3]. The region-based metrics include the *Jaccard* coefficient, widely used to measure spatial overlap, as well as Dice false positives (*Dice FP*) and Dice false negatives (*Dice FN*). *Dice FP* assesses over-segmentation and *Dice FN* under-segmentation. As contour-based metrics, we use the *Hausdorff* distance and the Mean Absolute contour Distance (*MAD*). To assess the performance of splitting, as in [3], we employ the number of false positives (*FP*) that counts the spuriously segmented cells and the number of false negatives (*FN*) that counts the cells that have not been segmented.

Experimental results: The proposed method is compared with top performing methods, namely, the *Three-step* [11], the *LSBR* [10], the *LLBWIP* [3]) and the *Otsu* method with a hole filling step as described in [6]. Tables 1 and 2 summarize the results obtained on the *U20S* and *NIH3T3* datasets, respectively. Tables present average scores computed over individual scores per image of a dataset. On the U20S dataset, *SEG-SELF* and *LLBWIP* yield similar results, outperforming the rest of the methods. *SEG-SELF* clearly outperforms all the methods under any metric in the more challenging *NIH3T3* dataset, due to the proposed adaptive image segmentation method that give high performance results under variations on background and foreground brightness. Table 3 gives the evaluation of splitting results on the *U20S* and *NIH3T3* datasets, where the performances of the methods agree with the segmentation performances.

[1]The code implementing the proposed method together with experimental results are publicly available in https://sites.google.com/site/costaspanagiotakis/research/cs.

Table 3. Splitting results on the **U20S** and **NIH3T3** datasets.

Methods	U20S		NIH3T3	
	FP	FN	FP	FN
Three-step	0.5	3.9	1.7	11.3
LLBWIP	**0.3**	2.7	1.5	5.0
SEG-SELF	2.7	**0.3**	**0.7**	**0.8**

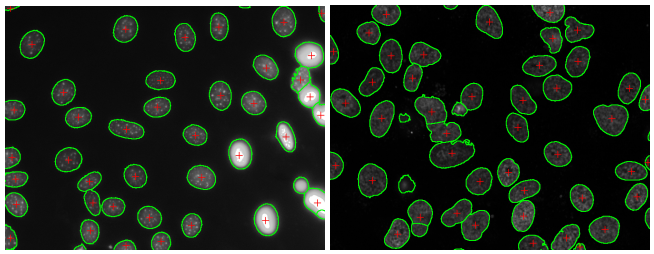

Fig. 3. Sample results of the *SEG-SELF* method on the *NIH3T3* (left) and *U20S* (right) datasets.

Qualitative results: Figure 3 shows two sample, representative results of the proposed method. In both cases, the *SEG-SELF* method successfully recognizes and correctly splits the high majority of cells, even if there exist important variations on cell size, shape and intensity.

4. SUMMARY

We proposed a method for accurate and automatic segmentation of cells that may touch each other. An initial segmentation of cell nuclei is performed with an extension of Bradleys method [16]. The segmentation of the touching cells has been achieved by employing an extension of an existing solution to the problem of multi-ellipse fitting presented in [17]. The experimental results on challenging public datasets showed the effectiveness of the proposed method as well as its superiority in comparison to relevant state-of-the-art methods.

5. REFERENCES

[1] Costas Panagiotakis, Ilias Grinias, and Georgios Tziritas, "Natural image segmentation based on tree equipartition, bayesian flooding and region merging," *IEEE Transactions on Image Processing*, vol. 20, no. 8, pp. 2276–2287, 2011. 1

[2] Costas Panagiotakis, Harris Papadakis, Elias Grinias, Nikos Komodakis, Paraskevi Fragopoulou, and Georgios Tziritas, "Interactive image segmentation based on synthetic graph coordinates," *Pattern Recognition*, vol. 46, no. 11, pp. 2940–2952, 2013. 1

[3] Amin Gharipour and Alan Wee-Chung Liew, "Segmentation of cell nuclei in fluorescence microscopy images: An integrated framework using level set segmentation and touching-cell splitting," *Pattern Recognition*, vol. 58, pp. 1–11, 2016. 1, 2, 4

[4] Wanjun Zhang and Huiqi Li, "Automated segmentation of overlapped nuclei using concave point detection and segment grouping," *Pattern Recognition*, vol. 71, pp. 349–360, 2017. 1, 2

[5] Nobuyuki Otsu, "A threshold selection method from gray-level histograms," *IEEE Transactions on Systems, Man, and Cybernetics*, vol. 9, no. 1, pp. 62–66, 1979. 1, 2

[6] Miao Liao, Yu-qian Zhao, Xiang-hua Li, Pei-shan Dai, Xiao-wen Xu, Jun-kai Zhang, and Bei-ji Zou, "Automatic segmentation for cell images based on bottleneck detection and ellipse fitting," *Neurocomputing*, vol. 173, pp. 615–622, 2016. 1, 2, 4

[7] Hai Su, Fuyong Xing, Jonah D Lee, Charlotte A Peterson, and Lin Yang, "Automatic myonuclear detection in isolated single muscle fibers using robust ellipse fitting and sparse representation," *IEEE/ACM Transactions on Computational Biology and Bioinformatics (TCBB)*, vol. 11, no. 4, pp. 714–726, 2014. 1

[8] Xiangzhi Bai, Changming Sun, and Fugen Zhou, "Splitting touching cells based on concave points and ellipse fitting," *Pattern Recognition*, vol. 42, no. 11, pp. 2434–2446, 2009. 1, 2

[9] Costas Panagiotakis, Emmanuel Ramasso, and Georgios Tziritas, "Lymphocyte segmentation using the transferable belief model," in *Recognizing Patterns in Signals, Speech, Images and Videos*, pp. 253–262. Springer, 2010. 1, 2

[10] Yao-Tien Chen, "A level set method based on the bayesian risk for medical image segmentation," *Pattern Recognition*, vol. 43, no. 11, pp. 3699–3711, 2010. 1, 4

[11] Jan Philip Bergeest and Karl Rohr, "Efficient globally optimal segmentation of cells in fluorescence microscopy images using level sets and convex energy functionals," *Medical Image Analysis*, vol. 16, no. 7, pp. 1436–1444, 2012. 1, 4

[12] Carolina Wählby, Joakim Lindblad, Mikael Vondrus, Ewert Bengtsson, and Lennart Björkesten, "Algorithms for cytoplasm segmentation of fluorescence labelled cells," *Analytical Cellular Pathology*, vol. 24, no. 2-3, pp. 101–111, 2002. 2

[13] Chanho Jung and Changick Kim, "Segmenting clustered nuclei using h-minima transform-based marker extraction and contour parameterization," *IEEE Transactions on Biomedical Engineering*, vol. 57, no. 10, pp. 2600–2604, 2010. 2

[14] Wen-Hui Zhang, Xiaoya Jiang, and Yin-Mingzi Liu, "A method for recognizing overlapping elliptical bubbles in bubble image," *Pattern Recognition Letters*, vol. 33, no. 12, pp. 1543–1548, 2012. 2

[15] Michele Fornaciari, Andrea Prati, and Rita Cucchiara, "A fast and effective ellipse detector for embedded vision applications," *Pattern Recognition*, vol. 47, no. 11, pp. 3693–3708, 2014. 2

[16] Derek Bradley and Gerhard Roth, "Adaptive thresholding using the integral image," *Journal of Graphics Tools*, vol. 12, no. 2, pp. 13–21, 2007. 2, 3, 4

[17] Costas Panagiotakis and Antonis Argyros, "Parameter-free modelling of 2d shapes with ellipses," *Pattern Recognition*, vol. 53, pp. 259–275, 2016. 2, 3, 4

[18] I. Kåsa, "A circle fitting procedure and its error analysis," *IEEE Transactions on Instrumentation and Measurement*, vol. 1001, no. 1, pp. 8–14, 1976. 2

[19] Euisun Choi and Chulhee Lee, "Feature extraction based on the bhattacharyya distance," *Pattern Recognition*, vol. 36, no. 8, pp. 1703–1709, 2003. 3

[20] Spyros Liapis and Georgios Tziritas, "Color and texture image retrieval using chromaticity histograms and wavelet frames," *IEEE Transactions on Multimedia*, vol. 6, no. 5, pp. 676–686, 2004. 3

[21] Guy Barrett Coleman and Harry C Andrews, "Image segmentation by clustering," *Proceedings of the IEEE*, vol. 67, no. 5, pp. 773–785, 1979. 3

[22] Luís Pedro Coelho, Aabid Shariff, and Robert F. Murphy, "Nuclear segmentation in microscope cell images: A hand-segmented dataset and comparison of algorithms," in *Proceedings - 2009 IEEE International Symposium on Biomedical Imaging: From Nano to Macro, ISBI 2009*, 2009. 4